Persistent photoinduced modifications in the phase-separated states of $La_{2-2x}Sr_{1+2x}Mn_2O_7$

Kai Sun,[1,3] Shuaishuai Sun,[1] Xingyuan Li,[1] Zhongwen Li,[1] Ruixin Zhang,[1] Linlin Wei,[1] Cong Guo,[1] Dingguo Zheng,[1] Huanfang Tian,[1] Huaixin Yang,[1,3] and Jianqi Li[1,2,3,*]

[1]*Beijing National Laboratory for Condensed Matter Physics, Institute of Physics, Chinese Academy of Sciences, Beijing 100190, China*

[2]*Collaborative Innovation Center of Quantum Matter, Beijing 100190, China*

[3]*School of Physical Sciences, University of Chinese Academy of Sciences, Beijing 100049, China*

(Received 6 May 2016; revised manuscript received 17 October 2016; published 4 November 2016)

Reentrant charge-ordering transition (RCOT) in the bilayered perovskite manganite $La_{2-2x}Sr_{1+2x}Mn_2O_7$ can yield observable changes in both the structural and physical properties associated with phase separation. Our recent measurements show that laser illumination can result in persistent modifications of both the resistance and microstructure in the phase-separated (PS) states. Measurements of photoinduced effects on an $x = 0.6$ sample reveal a persistent increase of the resistance by as much as 40%. Low-temperature laser *in situ* transmission electron microscope observations clearly show that *in situ* laser irradiation can modify the PS nature and strengthen the charge-ordered state. We attribute these photoinduced phenomena to the optical modulation of the hole concentration in the MnO_2 layers and the alteration of the local Mn orbital configurations in the PS states.

DOI: 10.1103/PhysRevB.94.205108

I. INTRODUCTION

Transition-metal oxides with perovskite structures show a rich variety of physical properties, including the colossal magnetoresistance (CMR) effect, charge-ordering (CO) transition, and phase-separated (PS) states [1–4]. The layered perovskite family $(La,Sr)_{n+1}Mn_nO_{3n+1}$, where $n = 1, 2$, and ∞ [1,5,6], has attracted much attention in the past decades as a result of the discovery of remarkable physical and structural phenomena arising from the interplay of charge, orbital, spin, and lattice degrees of freedom. Structural and physical measurements on the $n = 2$ layered materials revealed a reentrant charge-ordering transition (RCOT) associated with the PS states in $La_{2-2x}Sr_{1+2x}Mn_2O_7$ ($0.5 < x < 0.75$) [3,4,7]. However, it was also noted that the CO and magnetic states can be modulated (modified) by a variety of external stimuli such as magnetic fields [1], x-ray irradiation [8], and laser illumination [9–11]. Recently, photoinduced modifications of physical properties have attracted great interest because of their significant potential for understanding the fundamental mechanism underlying the complex nature of strongly correlated oxides, e.g., the x-ray–induced transition from an antiferromagnetic (AFM) insulator to the metallic ferromagnetic (FM) state in $(Pr,Ca)MnO_3$ [8] and the persistent photoconductivity in a Cr-doped $Pr_{0.5}Ca_{0.5}MnO_3$ film [12]. In particular, the rapid rise of ultrafast technology has led to the development of new means of revealing the complicated dynamics of spin [13], orbital order [14], electronic structure [15], and other features. In this paper, we report the photoinduced effects in the PS state for the double-layered manganite $La_{2-2x}Sr_{1+2x}Mn_2O_7$, in which a persistent photoinduced resistance change was found to exist in the PS states. To address the relevant microstructure changes, we obtained transmission electron microscope (TEM) images under *in situ* laser irradiation at low temperatures.

II. EXPERIMENT

A well-characterized polycrystalline sample with $x = 0.6$ and a single-crystal sample with $x = 0.5$ were used in the present study [16]. Figure 1(a) shows a schematic diagram of the resistivity measurements for the $La_{2-2x}Sr_{1+2x}Mn_2O_7$ samples under laser irradiation. The laser beam was derived from an 8-kHz (repetition rate) laser source (355 nm) with a pulse length of 7.7 ns and a laser output power of 100 mW. The samples used for photoinduced resistance measurements were adhered to a silicon substrate with dimensions of approximately $2 \times 2 \times 0.1$ mm^3. Four electrodes on one side of the sample were steadily fixed using silver paint with a gap between each electrode of approximately 600 μm, as shown in Fig. 1(a). The resistances were obtained by the conventional four-probe method. *In situ* TEM investigations were performed using a four-dimensional ultrafast transmission electron microscope equipped with a cooling holder [17].

III. RESULTS AND DISCUSSION

In previous studies, the magnetic properties and relevant microstructure features of bilayer manganite $La_{2-2x}Sr_{1+2x}Mn_2O_7$ ($0.45 \leqslant x \leqslant 0.67$) have been extensively investigated for correlation with low-temperature PS states and CO transitions [5,7,16]. Figure 1(b) shows the temperature dependence of the resistance as measured for several polycrystalline samples [7]; for comparison, the data obtained from a single crystal are also discussed as follows. The resistance upturns, indicated by arrows, show the onsets of the CO transition and melting. The critical temperature, T_{co}, increases strongly with Sr substitution for La. The reentrant CO melting results in clear decreases in the resistance, as analyzed in Ref. [7]. The structural and magnetic measurements revealed a remarkable reentrant CO melting associated with the PS state that could yield complex changes of CO states and magnetic structures [7,16]. In the present study, our investigation focuses on the sample with $x = 0.6$, which shows an abrupt resistance alteration at approximately 180 K and obvious reentrant CO melting at lower temperatures [5,16,18].

*Corresponding author: ljq@aphy.iphy.ac.cn

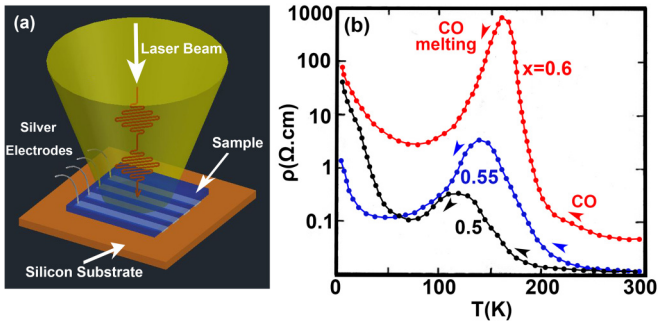

FIG. 1. (a) Schematic of the experimental setup; a sample on the silicon substrate is used for resistance measurements. Laser pulses are illuminated on the front of the sample, and four electrodes are attached to the back of the sample. (b) Temperature dependence of resistivity for $La_{2-2x}Sr_{1+2x}Mn_2O_7$ with $x = 0.5, 0.55$, and 0.6.

For the photoinduced changes in the $La_{2-2x}Sr_{1+2x}Mn_2O_7$ samples, it is known that the photoillumination effect depends strongly on the charge/orbital ordered state and PS nature, as discussed in Refs. [11,12]. Therefore, we performed our experimental measurements on the $x = 0.6$ sample at different temperatures below the CO transition temperature. Figures 2(a)–2(c) display the time dependence of the resistance changes caused by the laser illumination for the three temperatures corresponding to the (A) CO, (B) CO melting, and (C) AFM states in Fig. 2(e). In these experimental measurements, each datum was obtained after laser illumination for approximately 5 min. The resistance was observed to decrease immediately along with the laser illumination due to the appearance of photoexcited charge carriers, i.e., the transient photoconductivity, as shown in Fig. 2(e) [19]. The photoinduced resistance changes clearly show different features at different temperatures. For instance, in Fig. 2(e), the resistances at (A) the CO state at 175 K and (C) the AFM state at 51 K nearly return to the original values obtained prior to laser illumination. However, it is remarkable that at (B) 118 K and (D) 133 K, corresponding to reentrant CO melting (in PS states), the laser irradiation could induce high-resistance states in the sample, as also indicated in Fig. 2(e). Importantly, based on our experimental measurements, the relaxation processes of these resultant high-resistance states can take longer than two days at room temperature, i.e., the resistance does not regain the initial value but rather remains in the different state with a higher resistance, as illustrated in Fig. S1 in the Supplemental Material [20]. To completely reach the ground states for the next laser illumination experiment, the samples must either be deposited at room temperature for more than a week or annealed at 400 °C for 1 h, as confirmed in our experiments.

The photoinduced effects were also found to depend not only on temperature but also on the laser fluence. Therefore, we performed experimental measurements on the $x = 0.6$ sample for different illumination times. Figure 2(d) shows the resistance changes following photoexcitation, with the illumination time ranging from 30 s to 360 s. When the laser irradiation time was less than 120 s, higher laser fluences were used, and a higher resistance state could be achieved. However, if the illumination time was longer than 3 min, the photoinduced changes showed a notable saturation tendency. This fact suggests that the distribution and dynamic motion of the photoinduced charge carriers immediately reach the excited states under illumination, and then, it takes more than

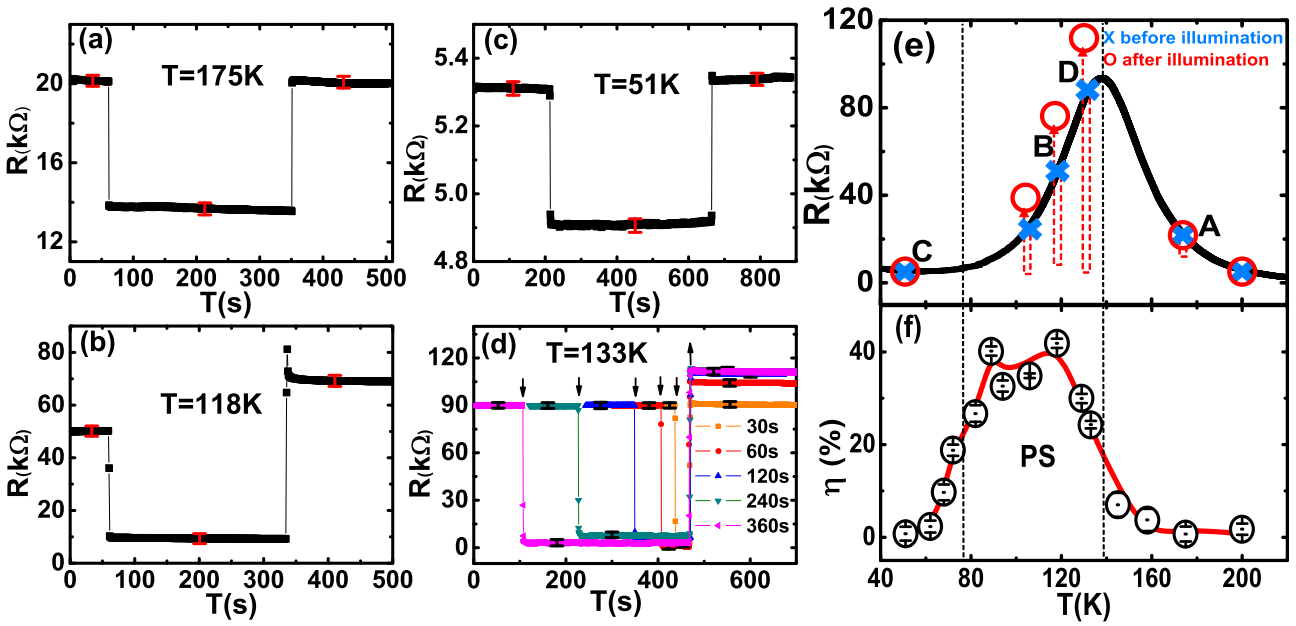

FIG. 2. (a)–(c) Time dependence of resistance changes caused by laser illumination for an $x = 0.6$ sample at (a) 175 K, (b) 118 K, and (c) 51 K. (d) Time dependence of resistance under different illumination times at 133 K; start and end points are indicated by "↓" and "↑" arrows, respectively. Standard deviation values are indicated by error bars. (e) Photoinduced resistance changes at different temperatures, illustrating that the persistent modifications appear for PS states. (f) Rate of resistance change, $\eta = \Delta R_T/R_T$, obtained in our experimental measurements at different temperatures for the $x = 0.6$ sample; here, R_T is the resistance of the sample at temperature T and ΔR_T is the photoinduced change of R_T. Noticeable changes are observed for the PS states.

3 min for the phase-separated state to evolve and reach a novel equilibrium state under our experimental conditions. Therefore, to study the essential features of the persistent photoinduced effects in this layered material, all samples in our study were initially illuminated for 5 min.

Figure 2(f) shows the resistance changes (as a percentage) of the $x = 0.6$ sample arising from laser illumination between 40 K and 200 K. This resistance is measured by the parameter $\eta = \Delta R_T/R_T$, where R_T is the resistance of the sample at temperature T and ΔR_T is the photoinduced change of R_T. Photoinduced persistent resistance increases are observed to occur only in the reentrant CO melting process, in which phase separation has been observed in the temperature range from 140 K to 80 K [7]. The maximum η was found to be ~40% at 118 K. This remarkable effect is believed to be correlated with the competition between the CO and AFM states. In contrast, our measurements show that the photoinduced resistance changes occurring in other temperature ranges, including those corresponding to the CO and AFM states, are completely reversible, and the observed resistance changes are well understood by the appearance of transient photoconductivity. Thus, the resistance can immediately return to the initial state when the laser beam is turned off.

It is commonly known that laser irradiation can lead to the coexistence of heating and optical effects in experimental data. Therefore, it is often suspected that certain experimental phenomena are potentially caused by laser heating. To identify the photoinduced changes in the present system, we performed a careful analysis of the experimental results obtained under different conditions. For instance, when the laser illumination was applied to the $x = 0.6$ sample at 133 K, the resistance increased rapidly to over 110 kΩ, as shown in Figs. 2(d) and 2(e). If the resistance change is attributed to the rise in the sample temperature, it is impossible to believe that the sample resistance can exceed the maximum resistance of 90 kΩ shown in the $R - T$ curve of Fig. 2(e). Therefore, we can conclude that the heating effect during laser illumination is certainly limited in yielding the persistent changes discussed above. Moreover, to minimize the heating errors in our measurements, we always maintained a steady experimental temperature and the resistance data were obtained after the laser had been turned off for at least 3 min. In fact, the photoinduced high resistance could persist for an extended period of time (more than 2 days), as has been similarly reported in Refs. [21,22].

To better understand the microstructural changes associated with these photoinduced phenomena, we performed *in situ* TEM examinations of the laser-illuminated $La_{2-2x}Sr_{1+2x}Mn_2O_7$ samples. Our microstructure analysis focused on the change of the CO state and domain structures at low temperatures for samples with $0.5 \leqslant x \leqslant 0.67$. The corresponding schematic view of charge and orbital ordering in the present layered system is displayed in Fig. S2 [20], as discussed in Refs. [5,16]. TEM observations clearly demonstrate that the CO domains often show clear evolution following the *in situ* laser illumination in the PS states.

Dark-field imaging from the superstructure spot appears to be the most suitable technique for studying the spatial inhomogeneity of the CO state in the phase-separated states [5,7]. Figures 3(a) and 3(b) present the dark-field TEM images of the $x = 0.6$ sample at an identical position obtained before and after laser illumination, respectively. (The original TEM images are shown in Fig. S3 [20].) These images were obtained using one of the satellite spots (i.e., the circled spot) of the (020) main diffraction spot, illustrating the CO domain structures at 115 K. The complex contrast can be explained directly as the coexistence of charge-ordered bright speckles and charge-disordered dark speckles [5,7]. Figure 3(c) exhibits an electron diffraction pattern obtained along the [001] zone-axis direction, in which the satellite spots are well assigned to an incommensurate CO modulation [7]. Figure 3(b) exhibits the visible changes of the spatial contrast variations, especially in the central region of the original image. Obviously, the laser illumination drives the original PS state with sparse CO lamella to an apparently dense CO cluster. Figure 3(d) displays the contrast difference between the dark-field TEM images before and after illumination, as obtained by a subtraction operation of Figs. 3(b) and 3(a), confirming the spatial variation of the CO state arising from the laser illumination. The CO lamellas are demonstrated to increase predominantly as a result of the photoinduced effect and reconstruction of CO domains, which can be well interpreted as the increase of the CO fraction in the PS state. Moreover, electron energy loss spectroscopy (EELS) and *in situ* electron diffraction observations were used to check the sample before and after illumination (shown in Figs. S4 and S5 [20]), clearly showing that no chemical shifts

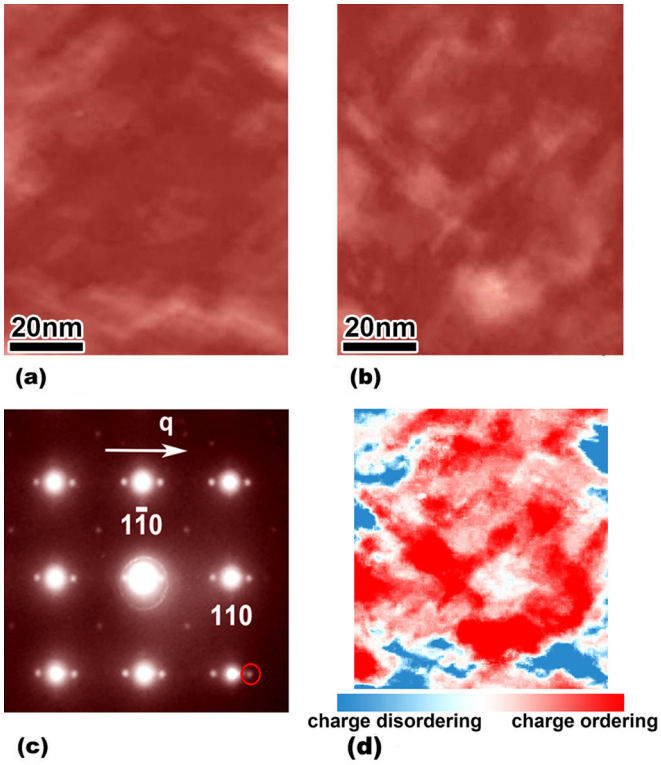

FIG. 3. Dark-field images for an $x = 0.6$ crystal obtained by *in situ* TEM observations at 115 K (a) before and (b) after laser illumination. (c) [001] zone-axis electron diffraction pattern of the $x = 0.6$ sample obtained at 115 K. Clear satellite spots following the basic diffraction spots arise from the CO modulations; the cycled satellite spot is used for *in situ* imaging. (d) Image of contrast difference between Figs. 3(a) and 3(b), clearly demonstrating the growth of the CO domains.

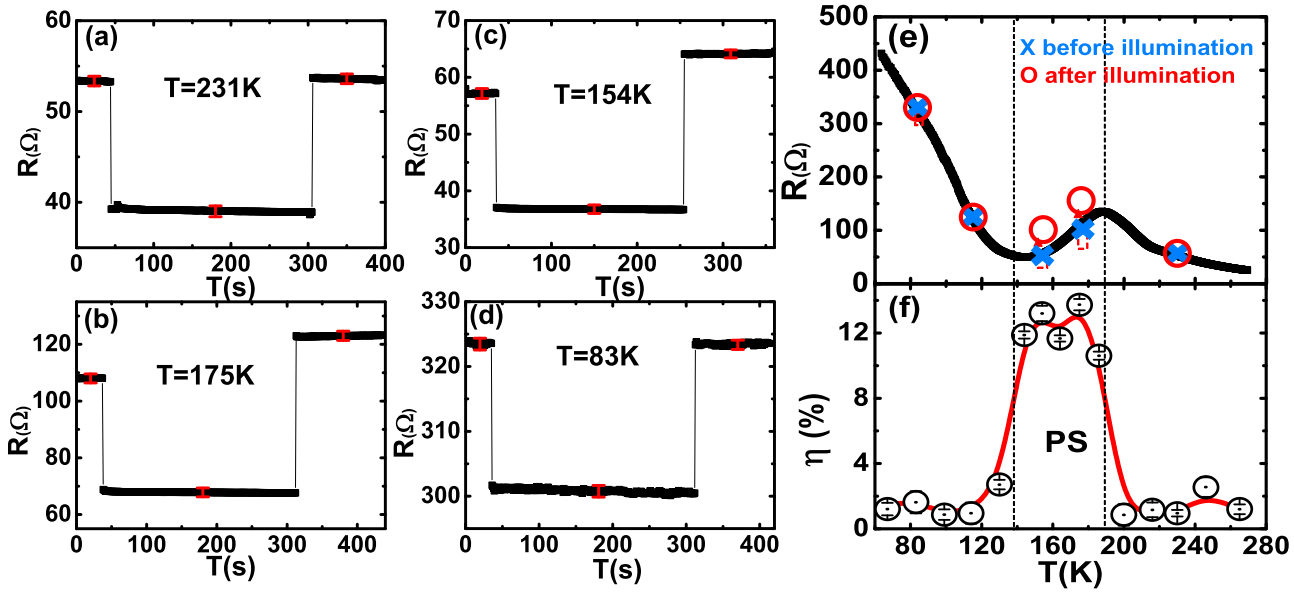

FIG. 4. (a)–(d) Photoinduced resistance changes for a single-crystal sample with $x = 0.5$ at (a) 231 K, (b) 175 K, (c) 154 K, and (d) 83 K. Error bars represent the standard deviation of the resistance drift arising from temperature fluctuations. (e) Photoinduced resistance alterations measured at different temperatures, where persistent modifications appear only for PS states. (f) Rate of resistance change, $\eta = \Delta R_T/R_T$, obtained in experimental measurements at different temperatures for the $x = 0.5$ sample, demonstrating clear resistance increases in the PS states.

and structural changes can be observed in the illuminated samples.

Furthermore, we performed the photoinduced measurements in a single crystal with $x = 0.5$, for which similar phenomena were observed, as shown in Fig. 4. This sample has been previously used for magnetic and structural studies, as reported in Refs. [5,6]. Figure 4(e) shows the resistance curve as a function of temperature as measured in the a-b plane. The onset point of the CO transition is at approximately 220 K, and the PS states occur in the temperature range from ~190 to ~140 K. The resistance curve exhibits a broad peak centered at 190 K that decreases progressively with lower temperature as a result of CO suppression [16]. Figures 4(a)–4(d) show the time dependence of the resistance changes caused by the laser illumination at four temperature points, summarized in Fig. 4(e). Similar to what was observed for the $x = 0.6$ sample, the persistent photoinduced alteration of the resistance in the $x = 0.5$ crystal occurs only in the PS states, as indicated in Fig. 4(f). However, the η value for the $x = 0.5$ sample, estimated to be approximately 10%, is smaller than that obtained for $x = 0.6$. This difference can be attributed to the changes in the strength of the interplay between the CO and magnetic ordering with decreasing doping content x [7].

The mechanism for photoinduced effects in strongly correlated systems, such as the photodoping scenario in high-T_c superconductors [22] and photoinduced charge/orbital switching in manganites [11], has been widely investigated in previous studies. Similar to chemical doping, photodoping can have a significant impact on the phase evolution via photocarrier-mediated electron doping or hole doping [22,23]. In the present study, the ultraviolet photons (3.5 eV) have sufficient energy for increasing the concentration of itinerant holes (or electrons) and modifying the occupation of the Mn orbital states; this can give rise to the reconfiguration of the Mn orbital ordered states and affect the local magnetic structure. In the bilayered $La_{2-2x}Sr_{1+2x}Mn_2O_7$ material, the CO state is associated with a staggered $d_{3x^2-r^2}/d_{3y^2-r^2}$ orbital ordering of the Mn^{3+}, and the layered type-A AFM state accompanies the uniform $d_{x^2-y^2}$ orbital ordering. As observed in our *in situ* TEM observations of the PS state, switching of the Mn^{3+} orbital-ordered state indeed occurred from $d_{x^2-y^2}$ to $d_{3x^2-r^2}/d_{3y^2-r^2}$ following the *in situ* laser illumination, and the nanometer CO domains increased visibly in the PS states [7,16].

On the other hand, the complicated magnetic ground states of the bilayered manganite can also be affected by the appearance of local magnetic disorders and oxygen vacancies. Photoillumination can trigger a notable perturbation of the local magnetic structure and result in the transformation of the orbital-ordered state; additionally, the phase separation in this layered system often accompanies the coexistence of the FM short-range ordering within the MnO_2 plane and the AFM coupling between the MnO_2 layers [6,16,24]. We measured the magnetization for single-crystal $La_{2-2x}Sr_{1+2x}Mn_2O_7$ ($x = 0.5$) before and after illumination. Indeed, a notable increase in the magnetization was observed, as shown in Fig. S6 [20]. This change could be caused essentially by charge transfer excitation from the $2p$ (O) to $3d$ (Mn) states. For instance, photoinduced superconductivity in $YBa_2Cu_3O_{7-x}$ has been previously discussed in the literature, with the photoexcited charge carriers believed to be partially trapped at the oxygen vacancies [25], preventing immediate annihilation of the charge carriers. In $La_{2-2x}Sr_{1+2x}Mn_2O_7$, the photogenerated holes can transfer to the MnO_2 layers following the laser being turned off, and a redistribution of the hole density through the hybridization of the p-d orbitals is certainly possible;

this is expected to increase the ferromagnetic interactions [23], contributing to the growth of the local short-range FM ordering and thus resulting in observable alterations of the local magnetic structure.

IV. CONCLUSION

In conclusion, persistent photoinduced modifications of the electrical resistance and microstructure in the bilayered manganites $La_{2-2x}Sr_{1+2x}Mn_2O_7$ ($x = 0.5$ and 0.6) have been found for the PS states associated with the reentrant CO transition. The largest resistance increase of ∼40% was observed in the $x = 0.6$ sample at a temperature of 118 K. Laser irradiation effects in the CO and AFM states emerged as reversible transitions that were well interpreted through the appearance of transient photoconductivity during experimental measurements. Moreover, microstructural changes of the CO nanodomains associated with laser illumination were directly revealed by *in situ* TEM observations at low temperatures. It is believed that the photoinduced modifications of the resistance and microstructure result from the optical modulation of the carrier concentration and local alteration of the Mn orbital configuration by injected high-energy photons.

ACKNOWLEDGMENTS

This work was supported by the National Basic Research Program of China 973 Program (No. 2015CB921300 and No. 2012CB821404), the National Key Research and Development Program of China (No. 2016YFA0300300), the Natural Science Foundation of China (Grants No. 11604372, No. 11274368, No. 51272277, No. 91221102, No. 11190022, No. 11474323, and No. 91422303), and the "Strategic Priority Research Program (B)" of the Chinese Academy of Sciences (No. XDB07020000).

[1] Y. Moritomo, A. Asamitsu, H. Kuwahara, and Y. Tokura, Nature (London) **380**, 141 (1996).
[2] T. Kimura, Y. Tomioka, H. Kuwahara, A. Asamitsu, M. Tamura, and Y. Tokura, Science **274**, 1698 (1996).
[3] A. Moreo, S. Yunoki, and E. Dagotto, Science **283**, 2034 (1999).
[4] G. Varelogiannis, Phys. Rev. Lett. **85**, 4172 (2000).
[5] J. Q. Li, Y. Matsui, T. Kimura, and Y. Tokura, Phys. Rev. B **57**, R3205 (1998).
[6] C. D. Ling, J. E. Millburn, J. F. Mitchell, D. N. Argyriou, J. Linton, and H. N. Bordallo, Phys. Rev. B **62**, 15096 (2000).
[7] J. Q. Li, C. Dong, L. H. Liu, and Y. M. Ni, Phys. Rev. B **64**, 174413 (2001).
[8] V. Kiryukhin, D. Casa, J.P. Hill, B. Keimer, A. Vigliante, Y. Tomioka, and Y. Tokura, Nature (London) **386**, 813 (1997).
[9] S. Majumdar, H. Huhtinen, M. Svedberg, P Paturi, S Granroth, and K Kooser, J. Phys.: Condens. Matter **23**, 466002 (2011).
[10] J. M. Dai, G. Y. Yuan, W. H. Song, and Y. P. Sun, Physica B **371**, 245 (2006).
[11] N. Takubo, I. Onishi, K. Takubo, T. Mizokawa, and K. Miyano, Phys. Rev. Lett. **101**, 177403 (2008).
[12] H. Oshima, M. Nakamura, and K. Miyano, Phys. Rev. B **63**, 075111 (2001).
[13] T. Ogasawara, M. Matsubara, Y. Tomioka, M. Kuwata-Gonokami, H. Okamoto, and Y. Tokura, Phys. Rev. B **68**, 180407 (2003).
[14] H. Ehrke, R. I. Tobey, S. Wall, S. A. Cavill, M. Forst, V. Khanna, Th. Garl, N. Stojanovic, D. Prabhakaran, A. T. Boothroyd, M. Gensch, A. Mirone, P. Reutler, A. Revcolevschi, S. S. Dhesi, and A. Cavalleri, Phys. Rev. Lett. **106**, 217401 (2011).
[15] L. Piazza, C. Ma, H. X. Yang, A. Mann, Y. Zhu, J. Q. Li, and F. Carbone, Struct. Dyn. **1**, 014501 (2014).
[16] T. Kimura, R. Kumai, Y. Tokura, J. Q. Li, and Y. Matsui, Phys. Rev. B **58**, 11081 (1998).
[17] S. S. Sun, L. L. Wei, Z. W. Li, G. L. Cao, Y. Liu, W. J. Lu, Y. P. Sun, H. F. Tian, H. X. Yang, and J. Q. Li, Phys. Rev. B **92**, 224303 (2015).
[18] Y. Okimoto, Y. Tomioka, Y. Onose, Y. Otsuka, and Y. Tokura, Phys. Rev. B **59**, 7401 (1999).
[19] G. Yu, C. H. Lee, A. J. Heeger, N. Herron, and E. M. McCarron, Phys. Rev. Lett. **67**, 2581 (1991).
[20] See Supplemental Material at http://link.aps.org/supplemental/10.1103/PhysRevB.94.205108 for further details of the experimental data and analyses.
[21] R. Cauro, A. Gilabert, J. P. Contour, R. Lyonnet, M.-G. Medici, J.-C. Grenet, C. Leighton, and Ivan K. Schuller, Phys. Rev. B **63**, 174423 (2001).
[22] V. I. Kudinov, I. L. Chaplygin, A. I. Kirilyuk, N. M. Kreines, R. Laiho, E. Lahderanta, and C. Ayache, Phys. Rev. B **47**, 9017 (1993).
[23] H. Huhtinen, R. Laiho, and V. Zakhvalinskii, Phys. Rev. B **71**, 132404 (2005).
[24] T. Kimura and Y. Tokura, Annu. Rev. Mater. Sci. **30**, 451 (2000).
[25] J. Hasen, D. Lederman, I. K. Schuller, V. Kudinov, M. Maenhoudt, and Y. Bruynseraede, Phys. Rev. B **51**, 1342 (1995).